INSIGHT INTO THE FISSION PROCESS FROM SURROGATE REACTIONS IN INVERSE KINEMATICS*

D. Ramos

GANIL, CEA/DRF-CNRS/IN2P3, BP 55027, 14076 Caen Cedex 5, France

(Received January 29, 2020)

Innovative experiments are conducted to widen our approach to fission, aiming notably at a complete identification and characterization of the fragments and the study of unstable fissioning systems. In the GANIL facility, full fission-fragment distributions and fragment kinetic energies are measured, thanks to the inverse kinematics technique and the magnetic spectrometer VAMOS. The access to the scission-point information is possible thanks to the low-energy regime. The initial excitation energy of the systems is also determined due to the well-defined transfer reactions. In this work, fission yields and fission-fragment kinetic energies of ^{239}U, as well as the evolution of the yields with the initial excitation energy of ^{240}Pu, are presented.

DOI:10.5506/APhysPolBSupp.13.499

1. Introduction

Several features of the nuclear matter interplay in the fission process and they determine the production of the resulting fission fragments [1]. For instance, the intrinsic structure of the nucleus plays an important role in fission at low energy because the asymmetric fission cannot be explained without taking into account structure effects [2]. At the same time, these fragment distributions cannot be understood without dynamical effects, such as dissipation, related to the nuclear matter viscosity that contributes to the reduction of the even–odd oscillation in the fission-fragment production [3].

The experimental access to observables that brings information about the different properties of the system is a very important step to constrain the state-of-the-art fission models. The continuous improvement in the detection equipments, together with the development of new techniques, such as the inverse kinematics and surrogate reactions, broaden the access either to more observables or to more exotic systems [4, 5].

* Presented at the XXVI Nuclear Physics Workshop *Key problems of nuclear physics*, Kazimierz Dolny, Poland, September 24–29, 2019.

The fission program running at VAMOS++/GANIL has contributed experimentally to the current knowledge on fission [6–13]. This fission program profits from the inverse kinematics using an intense uranium beam at low energy and from surrogate reactions to populate exotic fissioning systems through transfer and fusion reactions.

Here, we present some relevant results achieved within this program concerning the fission-fragment and kinetic-energy distributions of ^{239}U and ^{240}Pu.

2. Experimental setup

The measurements presented in this work were carried out at GANIL, where a beam of ^{238}U at $\sim$ 6 MeV/nucleon impinged on thin light targets — 500 μg/cm^2-^{9}Be and 100 μg/cm^2-^{12}C — in order to induce the fission of ^{239}U and ^{240}Pu through the transfer reactions ^{9}Be(^{238}U, ^{239}U)^{8}Be and ^{12}C(^{238}U,^{240}Pu)^{10}Be.

Once the transfer reaction takes place, the target-like recoil is emitted with polar angles around $\sim 40^\circ$ and both fragments are emitted at forward angles within a cone of $\sim 30^\circ$.

The target-like recoil is detected in a double-sided annular silicon telescope where it is isotopically identified. The telescope is segmented in order to measure the emission angles of the recoils and to reconstruct the binary reaction. Hence, the initial excitation energy of the fissioning system is determined event by event [7, 13]. The telescope geometry prevents the interception of the fission fragments.

For each fission event, one of the fragments passes through the VAMOS++ spectrometer [14] and it is fully identified at its focal plane setup in terms of nuclear charge, mass, ion charge-state, and velocity vector [15, 16].

For each fissioning system, the isotopic fission yields are determined taking into account the angular and momentum acceptance of the spectrometer as well as the detection efficiency. The velocity of the fission fragments in the center-of-mass reference frame is also determined by subtracting the kinetic boost introduced by the inverse kinematics [17].

3. Experimental results

The experimental results presented in the following concern the fission of two systems, ^{239}U and ^{240}Pu. In the case of ^{239}U, the full distribution of the measured excitation energy, from the fission barrier up to $\sim$ 10 MeV, is taken into account, resulting in a mean excitation energy of 8.3 MeV with a standard deviation of 2.7 MeV. In the case of ^{240}Pu, larger statistics allow us to explore the evolution of the system as a function of the excitation

energy by taking different ranges of the excitation-energy distribution as it is indicated in Table I, where the selected ranges, the mean values, and the standard deviations of each selection are presented.

TABLE I

List of the excitation energies selected in ^{240}Pu. Mean values, standard deviations, and ranges of excitation energy are presented.

$\langle E_x \rangle$ [MeV]	SD$_{E_x}$ [MeV]	E_x range [MeV]
8.5	1.46	[4.0–10.7]
9.5	1.32	[7.0–11.8]
10.5	1.46	[8.0–13.3]
11.5	1.63	[9.0–15.1]
12.5	1.79	[10.0–17.3]

3.1. Fission yields of ^{239}U

Figure 1 presents the fission yields of ^{239}U as a function of the proton (right) and neutron (left) content of the fragments. Present data (black dots) are compared with the GEF calculation [18]. For the first time, the neutron content of the fragments of ^{239}U is accessible by measuring simultaneously both, the atomic and the mass numbers of the fragments. Elemental fission yields from γ-spectroscopy are also presented (green triangles) [19]. Fission yields show a clear asymmetric fission with a very low population of intermediate elements. The agreement between present data and the GEF calculation is remarkable. The neutron distribution does not show mirror symmetry, contrary to the proton distribution, due to the neutron evap-

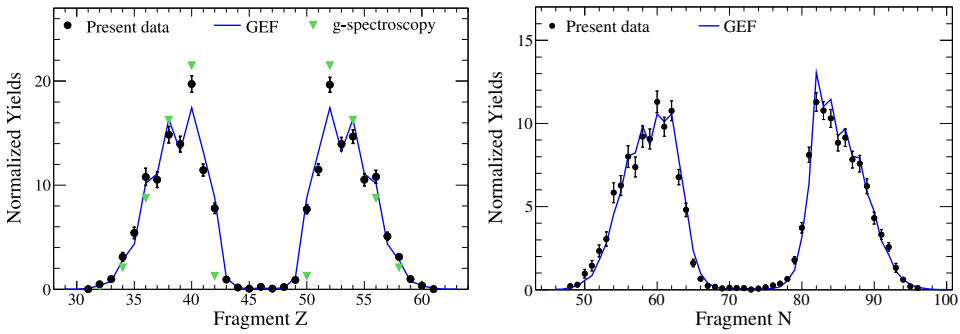


Fig. 1. (Colour on-line) Elemental (left panel) and isotonic (right panel) fission yields of ^{239}U. Present data (dots) are compared with the GEF calculation (line) [18] and with γ-spectroscopy measurements (green triangles) [19].

oration. Both distributions show a clear even–odd oscillation with larger production of even-Z and even-N nuclei. This oscillation is stronger in protons but it is still present in neutrons despite of the neutron evaporation.

3.2. Energetic balance at scission of ^{239}U

The measurement of the velocity vector of the fission fragments allows us to reconstruct the fragment velocity in the reference frame where the fissioning system is at rest ($v_{\rm cm}$). With this velocity, applying momentum conservation, the average mass of the fragments before neutron evaporation is determined as a function of the atomic number of the fragments ($\langle A_i^* \rangle$)

$$\langle A_1^* \rangle (Z_1) = A^{\rm FIS} \frac{\langle \gamma_{{\rm cm}_2} v_{{\rm cm}_2} \rangle (Z_2)}{\langle \gamma_{{\rm cm}_1} v_{{\rm cm}_1} \rangle (Z_1) + \langle \gamma_{{\rm cm}_2} v_{{\rm cm}_2} \rangle (Z_2)} , \quad (1)$$

$$\langle A_2^* \rangle (Z_2) = A^{\rm FIS} - \langle A_1^* \rangle (Z_1) , \quad (2)$$

where $\langle A_1^* \rangle + \langle A_2^* \rangle = A^{\rm FIS}$ is the mass of the fissioning system.

The total kinetic energy of the fission fragments at the scission point is obtained from those values

$$\langle {\rm TKE} \rangle (Z_1) = \langle {\rm TKE} \rangle (Z_2) = \langle M_1^* \rangle \left[\langle \gamma_{{\rm cm}_1} \rangle - 1 \right] (Z_1) + \langle M_2^* \rangle \left[\langle \gamma_{{\rm cm}_2} \rangle - 1 \right] (Z_2) . \quad (3)$$

Figure 2 (left) shows the $\langle {\rm TKE} \rangle$ of ^{239}U at scission as a function of the atomic number of the fission fragments. Present data (black dots) are compared with GEF (solid black/blue line) and with previous measurement from 1.8 MeV-n-induced fission (solid grey/green line) [20]. The $\langle {\rm TKE} \rangle$ is higher for $Z = 50$ splits than for larger asymmetries. This indicates that the scission elongation is shorter for $Z = 50$. Dotted and dashed lines represent the TKE for constant elongations at scission of 15.6 fm and 18.3 fm, respectively.

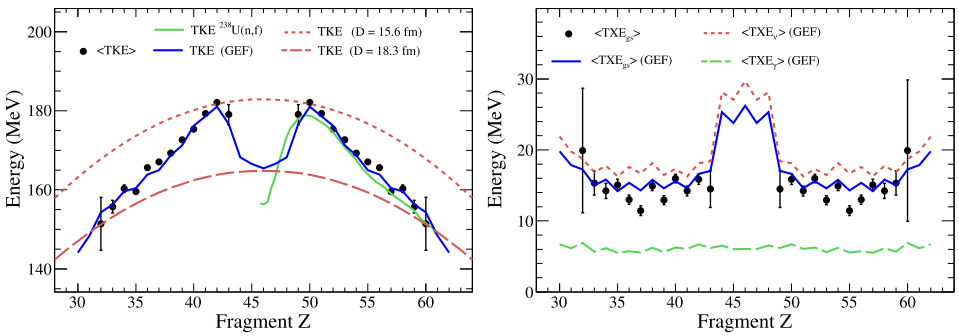


Fig. 2. (Colour on-line) Total kinetic energy (left panel) and total excitation energy (right panel) of the fission fragments of ^{239}U. See the text for details.

The difference between the reaction Q-value from the ground state of the fissioning system to the ground state of both fission fragments at scission and the TKE corresponds to the total excitation energy of the fragments at scission with respect to the ground state of the fissioning system ($\mathrm{TXE_{gs}}$). Figure 2 (right) presents the average $\mathrm{TXE_{gs}}$ of ^{239}U. Present data (black dots) are compared with the GEF calculation (solid blue line). The lack of statistics at symmetry prevents to prove experimentally the larger $\langle \mathrm{TXE_{gs}} \rangle$ predicted by GEF, while, in the asymmetric region, the $\langle \mathrm{TXE_{gs}} \rangle$ is rather constant. The TXE of the fragments is released through neutron and gamma evaporation. Both components are disentangled from GEF and they are also shown in the figure with dotted red and dashed green lines, respectively. The contribution of the neutron evaporation is more than 10 MeV larger than the one of gamma evaporation, predicted by GEF. In addition, the excess of TXE at symmetry can be explained through neutron evaporation, while the gamma-evaporation energy is rather constant in the full range.

3.3. Initial excitation-energy evolution of ^{240}Pu

The fission yields of ^{240}Pu are investigated as a function of the initial excitation energy of the system (E_x). The average values of the selected E_x ranges are indicated in Table I.

Figure 3 (left) presents the fission yields as a function of the fragment mass for different initial excitation energies. Present data, at two very different energies — 8.5 MeV and 12.5 MeV — are compared with previous measurements from neutron-induced fission at 6.5 MeV [21, 22]. There is clear feeding of symmetric fission by increasing E_x. The very asymmetric fission is also enhanced by higher E_x. Present and previous measurements are consistent with the evolution of E_x.

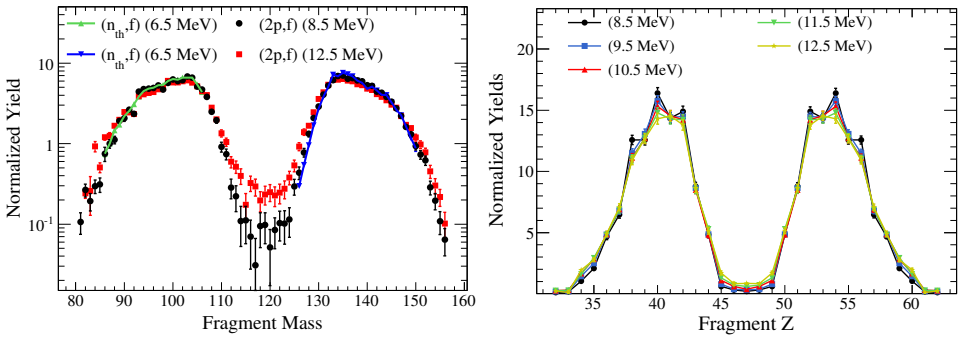


Fig. 3. Mass yields (left panel) and elemental yields (right panel) of ^{240}Pu for different excitation energies. Previous measurements from n_{th}-induced fission are also included [21, 22].

Figure 3 (right) shows the present fission yields as a function of the atomic number of the fragments. The 5 ranges of excitation energy selected are indicated by their mean value. A clear reduction of the even–odd oscillation is observed by increasing E_x. This can be understood as the increasing intrinsic excitation energy gradually reduces the pairing correlations.

Figure 4 shows the average total neutron multiplicity of ^{240}Pu as a function of the excitation energy. Present data (black dots) show lower neutron multiplicity than the previous measurement from neutron capture [23] (red squares). This difference can be produced by the different initial angular momentum of the fissioning system. The angular momentum introduced in the fissioning system is expected to be higher in the present data — 2-proton-transfer reaction in inverse kinematics — than in the direct neutron-capture reaction. Hence, higher states in rotational bands can be accessible from this transfer reaction more than from the neutron-capture reaction and this could favor the γ decay that competes with neutron evaporation.

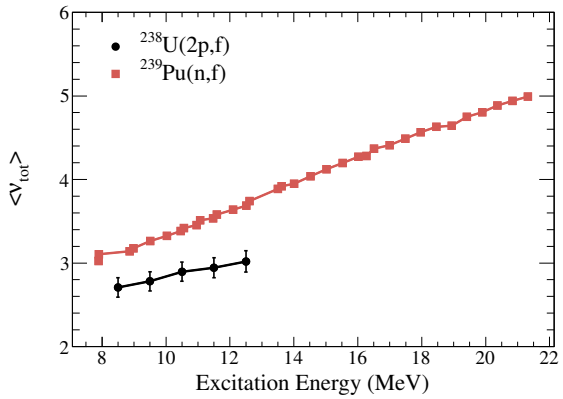


Fig. 4. (Colour on-line) Average total neutron multiplicity of ^{240}Pu as a function of the initial excitation energy. Present data (dots) are compared with a previous measurement from neutron-induced fission (squares) [23].

4. Conclusions

The fission yields of ^{239}U and ^{240}Pu are reported. Additional information concerning the fragment energies are obtained for ^{239}U and the impact of the initial excitation energy of the fissioning system was explored in ^{240}Pu.

A clear compact configuration at scission for the $Z = 50$ split was observed from the total kinetic energy, while the total excitation energy of the fragments remains constant in that region.

There is a clear feeding of the symmetric fission by increasing the initial excitation energy. The increasing excitation energy has also an impact on the rupture of proton pairs from the saddle to the scission point as it is observed in the reduction of the even–odd effect.

The average neutron multiplicity of the present data differs from that of a previous measurement from neutron-capture reactions. This difference could be explained in terms of the effect of the initial angular momentum.

In summary, the use of inverse kinematics with new experimental equipments gives the possibility to measure, simultaneously, a number of observables that were historically difficult to access, and the correlations between them provide new quantities sensitive to the fission properties.

REFERENCES

[1] K.-H. Schmidt, B. Jurado, *Rep. Prog. Phys.* **81**, 106301 (2018).
[2] G. Scamps, C. Simenel, *Nature* **564**, 382 (2018).
[3] F. Rejmund *et al.*, *Nucl. Phys. A* **678**, 215 (2000).
[4] K.-H. Schmidt *et al.*, *Nucl. Phys. A* **665**, 221 (2000).
[5] K. Nishio *et al.*, *Phys. Lett. B* **748**, 89 (2015).
[6] M. Caamaño *et al.*, *Phys. Rev. C* **88**, 024605 (2013).
[7] C. Rodríguez-Tajes *et al.*, *Phys. Rev. C* **89**, 024614 (2014).
[8] M. Caamaño *et al.*, *Phys. Rev. C* **92**, 034606 (2015).
[9] F. Farget *et al.*, *Eur. Phys. J. A* **51**, 175 (2015).
[10] M. Caamaño, F. Farget, *Phys. Lett. B* **770**, 72 (2017).
[11] D. Ramos *et al.*, *Phys. Rev. C* **97**, 054612 (2018).
[12] D. Ramos *et al.*, *Phys. Rev. C* **99**, 024615 (2019).
[13] D. Ramos *et al.*, *Phys. Rev. Lett.* **123**, 092503 (2019).
[14] M. Rejmund *et al.*, *Nucl. Instrum. Methods Phys. Res. A* **646**, 184 (2011).
[15] M. Vandebrouck *et al.*, *Nucl. Instrum. Methods Phys. Res. A* **812**, 112 (2016).
[16] Y. Kim *et al.*, *Eur. Phys. J. A* **53**, 162 (2017).
[17] D. Ramos, Ph.D. Thesis, University of Santiago de Compostela, 2016, http://hdl.handle.net/10347/15070
[18] K.-H. Schmidt *et al.*, *Nucl. Data Sheets* **131**, 107 (2016).
[19] J.N. Wilson *et al.*, *Phys. Rev. Lett.* **118**, 222501 (2017).
[20] F. Vivés *et al.*, *Nucl. Phys. A* **662**, 63 (2000).
[21] C. Schmitt *et al.*, *Nucl. Phys. A* **430**, 21 (1984).
[22] A. Bail *et al.*, *Phys. Rev. C* **84**, 034605 (2011).
[23] J. Frehaut, G. Mosinski, M. Soleilhac, private communication, 1980, EXFOR data base: https://www-nds.iaea.org/exfor/servlet/X4sGetSubent?reqx=2213&subID=20490003